



Published in final edited form as:

Ann Biomed Eng. 2017 November ; 45(11): 2548–2562. doi:10.1007/s10439-017-1899-0.

Proteomic alterations associated with biomechanical dysfunction are early processes in the *Emilin1* deficient mouse model of aortic valve disease

PM Angel¹, DA Narmoneva², MK Sewell-Loftin³, C Munjal⁴, L Dupuis⁵, BJ Landis⁶, A Jegga⁷, CB Kern⁵, WD Merryman³, HS Baldwin⁸, GM Bressan⁹, and RB Hinton⁴

¹Department of Cell and Molecular Pharmacology & Experimental Therapeutics, Medical University of South Carolina, Charleston, SC

²Division of Biomedical Engineering, University of Cincinnati, Cincinnati, OH

³Division of Biomedical Engineering Vanderbilt University, Nashville, TN

⁴Division of Pediatric Cardiology, Cincinnati Children's Hospital Medical Center, Cincinnati, OH

⁵Department of Regenerative Medicine, Medical University of South Carolina, Charleston, SC

⁶Division of Pediatric Cardiology, Indiana University, Indianapolis, IN

⁷Division of Biomedical Informatics, Vanderbilt University, Nashville, TN

⁸Division of Pediatric Cardiology, Vanderbilt University, Nashville, TN

⁹Department of Molecular Medicine, University of Padua, Padua

Abstract

Aortic valve (AV) disease involves stiffening of the AV cusp with progression characterized by inflammation, fibrosis, and calcification. Here, we examine the relationship between biomechanical valve function and proteomic changes before and after the development of AV pathology in the *Emilin1*^{-/-} mouse model of latent AV disease. Biomechanical studies were performed to quantify tissue stiffness at the macro (micropipette) and micro (atomic force microscopy (AFM)) levels. Micropipette studies showed that the *Emilin1*^{-/-} AV annulus and cusp regions demonstrated increased stiffness only after the onset of AV disease. AFM studies showed that the *Emilin1*^{-/-} cusp stiffens before the onset of AV disease and worsens with the onset of disease. Proteomes from AV cusps were investigated to identify protein functions, pathways, and interaction network alterations that occur with age- and genotype-related valve stiffening. Protein alterations due to *Emilin1* deficiency, including changes in pathways and functions, preceded biomechanical aberrations, resulting in marked depletion of extracellular matrix (ECM) proteins interacting with TGFB1, including latent transforming growth factor beta 3 (LTBP3), fibulin 5 (FBLN5), and cartilage intermediate layer protein 1 (CILP1). This study identifies proteomic

Correspondence: Robert B. Hinton, MD, Division of Cardiology, Cincinnati Children's Hospital Medical Center, 240 Albert Sabin Way, MLC 7020, Cincinnati, Ohio 45229. Fax: 513-636-5958. Phone: 513-636-0389. bingrbh@icloud.com.

Disclosures: None

dysregulation is associated with biomechanical dysfunction as early pathogenic processes in the *Emilin1*^{-/-} model of AV disease.

Key terms

valves; proteomics; biomechanics; aging; TGFbeta1; extracellular matrix; protein interaction networks

Introduction

Aortic valve (AV) disease affects over 2% of the world population.¹ Aging is an independent risk factor for AV disease, and as the general population ages, the incidence of disease increases.² AV disease is progressive, typically characterized by inflammation, fibrosis and calcification. These pathologic changes result in stiffening of the valve cusps obstructing forward blood flow (stenosis), and/or faulty closure of the valve cusps leading to backward blood flow (insufficiency). Patients with moderate to severe aortic valve stenosis develop cardiac dysfunction and heart failure, yet treatment is currently restricted to surgical or transcatheter aortic valve replacement.³ Identification of mechanisms that may provide therapeutic targets to treat early stages of AV disease are of critical importance; however, the regulation of AV disease initiation and progression is largely unknown.

Protein dysregulation is a key event in the pathological progression of AV disease. Changes in the content and organization of the extracellular matrix (ECM) structure are a primary cause of valve stiffening, and the resulting biomechanical abnormalities contribute to valve dysfunction.⁴ In healthy valve tissue, ECM is organized in a trilayer structure composed of collagens, glycosaminoglycans and elastic fibers as the result of a fetal developmental process.⁵ In diseased valve tissue, ECM loses its compartmentalization, becoming inflamed and calcified, and studies in mice have shown that these structural changes result in altered biomechanical properties.⁶⁻⁸ In human AV disease, proteomics on valve interstitial cells (VIC) demonstrated increased content of actin binding proteins.⁹ Likewise, proteomic evaluation of diseased human AV tissue showed significant changes in a number of proteins, including those involved in immune responses and inflammation.¹⁰ However, in humans, proteomic analyses are limited to end stage AV disease because of a lack of tissue availability, confounding analysis. Proteomic alterations associated with the progression of AV disease have not been explored.

Recently, we reported a new model of AV disease, the Elastin Microfibril Interfacer 1 deficient (*Emilin1*^{-/-}) mouse, which mimics the natural history of human AV disease.^{11,12} EMILIN1 is necessary for proper elastogenesis, and *Emilin1* deficiency results in latent hemodynamic AV disease in the majority of mice between 10–12 months of age, characterized in part by an early increase in p-Erk1/2 activation and late ECM disorganization and inflammation.^{12,13} Late-onset hemodynamic disease allows the distinction between early features of disease processes, before 6 months of age before hemodynamic disease, and advanced features of disease, after the manifestation of overt disease as heart failure. EMILIN1 inhibits TGFβ1 signaling¹⁴, and *Emilin1*^{-/-} AVs demonstrate both canonical (Smad2/3) and non-canonical (Erk1/2) TGFβ1 activation, as

well as fibrosis and inflammation, but not calcification.¹² *Emilin1*^{-/-} mice demonstrate a dynamic pathologic process that is characterized by early ECM changes and provides the opportunity to study disease progression. Understanding early disease processes is a priority in the heart valve community.¹⁵

The objective of this study was to examine AV biomechanics and protein networks before and after disease onset to further elucidate structure-function processes contributing to the progression of AV disease using the *Emilin1*^{-/-} mouse model. We hypothesized that *Emilin1* deficiency results in early proteomic alterations that precede AV disease and subsequent biomechanical dysfunction that occurs with disease. Global proteomic expression from mutant mice was interrogated before and after the manifestation of disease, and these findings were correlated with micro and macro biomechanical functional studies. This study provides new insight into mechanisms of early processes of AV disease and may contribute to the identification of new diagnostic and therapeutic approaches.

Methods

Animal groups

All animal use and handling was performed in accordance with protocols approved by the Cincinnati Children's Hospital Medical Center Institutional Animal Care and Use Committee. Mixed gender *Emilin1*^{-/-} mice and wild type (WT) littermates (*Emilin1*^{+/+}) were studied at adult (4–6 months) and aged (12–16 months). These time points were chosen as an early stage that preceded any disease and a late stage that manifested advanced disease, as described in previous work.¹² This resulted in four experimental groups: adult wild type (AdWT), aged wild type (AgWT), adult *Emilin1*^{-/-} (AdEM), and aged *Emilin1*^{-/-} (AgEM). We have presented genes and proteins according to the standards of nomenclature developed and maintained by the International Committee on Standardized Genetic Nomenclature for Mice (<http://www.informatics.jax.org/mgihome/nomen/>).

Dissection, histochemistry and immunohistochemistry

Dissection, histochemistry using a modified pentachrome stain, and immunohistochemistry were used to assess ECM content and organization, as previously described.^{6,8} See Supplemental Methods for details.

Macro biomechanical testing using micropipette aspiration

Regional biomechanical properties of *ex vivo* AV tissue were quantified using the micropipette approach that we developed recently.¹⁶ Ten mice per genotype per stage were studied. Briefly, the AV tissue was dissected to reveal cusp and annulus regions in situ, and mounted on a microscope slide. The valve surface was accessed from the ventricular side using a micromanipulator and glass micropipette with an inner diameter of 50–60 μm ; upon contact, aspiration pressure was applied in a step-wise manner, and an aspiration length was determined using image analysis of video frames.¹⁷ Pressure vs. aspiration length data were fit using linear regression. Young's modulus (E) as a measure of tissue stiffness was determined using a half-space model equation.^{18,19}

Microscale biomechanical testing using atomic force microscopy (AFM)

To quantify the microscale elastic modulus of the AVs, AFM testing was performed, as previously described.²⁰ Five mice per genotype per stage were studied. Briefly, adult and aged mice were sacrificed and whole hearts were excised into cold PBS. Samples were flash frozen without fixation in optimal cutting medium (OCT) and sectioned at 10 μm . Sections were prepared for AFM analysis by rinsing off the OCT in PBS, blocking with 10% FBS for 30 min, washing in PBS 3 \times , rinsing with dH_2O , and immediately subjected to AFM analysis. Scanning was completed on $30\mu\text{m} \times 30\mu\text{m}$ areas on valve cusp and annulus regions using borosilicate glass particle tips with a nominal diameter of $3\mu\text{m}$ and spring constant of 0.03N/m . The tip was calibrated to a 2.5MPa poly(dimethylsiloxane) standard prior to sample analysis. For each animal, scans were analyzed on each of five adjacent sections and a median modulus value was calculated for each scan. Median values were aggregated to calculate an average modulus for each animal, which was then used for statistical comparison.

Statistical analyses for biomechanical measurements

Multivariate ANOVA and post-hoc Bonferroni multiple comparison tests (SPSS Inc.) were used to determine effects by region (cusp, annulus), genotype (*Emilin1*^{-/-}, WT) and stage (adult, aged) on measures of tissue stiffness. All variables were reported as means \pm standard deviation. Differences were considered significant at $p < 0.05$.

Proteomic analysis

Protein was extracted from a pool of twelve AV cusps per experimental group and examined by proteomic methods, as described previously.²¹ Proteomics was performed on the excised cusp only. Annulus tissue is difficult to isolate by the microdissection methods needed for proteomic studies without introducing aortic wall tissue contamination. Excised cusps were decellularized using SDS detergent buffers, quantified using a bicinchoninic acid assay. A total of $60\ \mu\text{g}$ loaded onto a 12% Bis-Tris minigel (Invitrogen, Carlsbad, CA) and electrophoresed 15 minutes at 150 volts using MOPS-SDS running buffer, until high molecular weight marker (250 kDa) was approximately 0.4 cm below the well. Gel plugs were briefly stained (SimplyBlue SafeStain, Invitrogen, Grand Island NY) for protein visualization and each lane was minced into 1 mm cubes and treated by in-gel digestion, followed by peptide extraction using established protocols.²¹ Peptides were analyzed by inline multidimensional chromatography coupled to ion trap tandem mass spectrometry (LTQ, Thermo Scientific, Inc., San Jose, CA). Peptides were identified through database searching followed by clustering to proteins at 1% false discovery rate using ProteoIQ. Proteins that had greater than five spectral counts were used in quantitative comparisons. Comparative protein ratios were further filtered by significant ANOVA testing (p -value < 0.05) and ratios of ≥ 2 -fold. Further details are provided in the Supplemental Methods.

Bioinformatic analysis

Protein function and pathway enrichment were calculated by WebGestalt program comparing against KEGG and Wikipathways using a threshold of two fold enrichment and a corrected p -value $< 1.0\text{E-}3$ as a cutoff point.^{22,23} The term protein group enrichment

corresponds to the ratio of observed to expected number of genes from each proteome using the mouse genome as a reference set. Enrichment was calculated as the number of observed proteins compared to the expected number of proteins using the mouse genome as a reference. We have adopted the following approach to evaluating enrichment data: When a function or pathway is altered in the aged WT, but not the adult WT, it indicates the possible effect of aging. Further, a function or pathway may be altered in the adult mutant only (suggesting it is not an “aging” function), the aged mutant only (suggesting it is an “aging” function) or both the adult and aged mutant (suggesting it may or may not be an “aging” function). Significance of the ratio was calculated using a hypergeometric statistical method and was adjusted for multiple testing using the Benjamini-Hochberg correction.²⁴ Protein processes were evaluated using Ingenuity Pathways Analysis (IPA, QIAGEN Redwood City) v24390178 build 346717. A Comparison Analysis was used to calculate functions for each total proteome, filtered using a negative log *p*-value cutoff 3 as a threshold. Data were visualized using IPA or the TM4 Microarray Software Suite.²⁵

Results

Biomechanical testing shows macroscale AV tissue-level effects in aged *Emilin1*^{-/-} mice

Emilin1^{-/-} mice are a model of latent fibrotic AVD, exhibiting elastin fiber fragmentation and fibrosis, but do not demonstrate gross calcification or histopathologic mineralization.⁸ To examine the effect of the altered ECM on valve biomechanical properties contributing to valve dysfunction, we evaluated stiffness of the cusp and annulus during aging in *Emilin1*^{-/-} mice. A micropipette aspirate approach was used to determine Young’s modulus in the cusp and annulus regions of *Emilin1*^{-/-} and WT AVs at adult and aged stages (Figure 1), showing differential effects of aging by genotype. Between 4 and 12 months of age, *Emilin1*^{-/-} AV annulus stiffness increased 1.7 fold. Similarly, there was a significant 1.3 fold increase in *Emilin1*^{-/-} cusp stiffness measurements with age. In contrast, there was no significant difference in WT annulus or cusp stiffness values. Whole mount testing of AV stiffness therefore indicated that *Emilin1* deficiency results in increased stiffness in both annulus and cusp valve regions at the aged stage only.

AFM biomechanical microscale testing shows intrinsic ECM stiffening in the adult and aged *Emilin1* deficient AV, as well as the aged WT AV

Biomechanical testing using AFM was utilized to assess microstructural intrinsic properties of AV ECM (Figure 2). There was no significant difference in microstructural ECM properties between the WT and *Emilin1*^{-/-} AV annulus regions at either adult or aged stages (Figure 2A), although aged *Emilin1*^{-/-} trended towards increasing stiffness with high variation from animal to animal. In contrast, the AV cusp region of *Emilin1*^{-/-} mice showed a significant 1.4 fold increase in the micro-environmental stiffness between 4 and 12 months (Figure 2B). *Emilin1* deficiency resulted in a significant increase in microscale cusp stiffness in both adult and aged groups as compared to WT. Aging was associated with significant increases in microscale AV cusp stiffness in both *Emilin1*^{-/-} and WT mice (*p*-value 0.01). Cross sectional topography illustrated the subtle variation between the adult and aged WT, as well as a marked difference between the aged WT and aged *Emilin1*^{-/-} AV (Figure 2C). Therefore, *Emilin1* deficiency results in AV microstructure biomechanical stiffening in the

cusps before 4 months, prior to the development of macroscopic scale stiffening, which occurs between the ages of 4 and 12 months, and before hemodynamic AV disease.

***Emilin1* deficient AV proteomes show increased proportions of proteins involved in inflammation, angiogenesis and fibrosis**

In order to assess alterations in protein composition, we utilized a mass spectrometry based proteomics analysis. We first examined functions and pathways reported by global proteomes of adult and aged WT and *Emilin1*^{-/-} AV. When a function or pathway is reported altered in the aged WT, but not the adult WT, this function or pathway may be altered in the adult mutant only (suggesting it is not a function of aging), the aged mutant only (suggesting it is a function of aging) or both the adult and aged mutant (suggesting it may or may not be a function of aging). Clustering proteomes to functions revealed that whereas adult WT AVs showed no significant detection of fibrogenesis, the adult *Emilin1*^{-/-} AVs showed pro-fibrotic aberration of ECM, as did aged WT and aged *Emilin1*^{-/-} AVs (Figure 3A, Supplementary Table 1A). This is taken to illustrate that fibrogenesis is a normal process of aging and that ECM aberrations caused by *Emilin1* deficiency accelerate these processes. This is consistent with prior observations that ECM aberrations accelerate the effects of aging.²⁶ Enrichment of angiogenesis-related proteins was detected in all proteomes, with subtle changes in aged wild type and both *Emilin1*^{-/-} AVs (-log p-value of enrichment 21.2 AdWT; 25.5 AgWT; 25.4 AdEM; 23.3 AgEM, where Bonferroni corrected p-value 1.0E-3 was considered significant). We have previously reported that TGFβ1 mediates increases in angiogenesis during aging in the *Emilin1*^{-/-} mouse¹². The current data may be interpreted that at the global proteome level as follows: a subset of angiogenesis proteins are detectable at both stages, and another set of angiogenesis proteins are expressed at high levels in the aged *Emilin1* deficient mouse indicating similarities in disease development due to aging and in the *Emilin1*^{-/-} model. Interestingly, while “inflammatory response” appeared uniform across all proteomes, an increase with proteins involved in immune related processes of “adhesion of immune cells” and “cell movement of neutrophils” was observed in *Emilin1*^{-/-} valves. Immune cell infiltration, as evidenced by Mac-3 immunohistochemistry, has been previously demonstrated in the *Emilin1*^{-/-} aortic valve.^{12,27} Further investigation of proteins showed that ~15% overlap in proteins grouped to inflammation and immune response (Supplemental Table 1A), suggesting that these processes may be intertwined at the protein level in this model. Additionally, the function “connective tissue” was enriched in the *Emilin1*^{-/-} mice but not in the WT counterparts, and “morphology of cardiovascular tissue” was enriched in the aged *Emilin1*^{-/-} proteome (-log p-value 8.3) only, potentially reflecting the altered ECM protein content of increased tissue remodeling and increased cusp stiffness. Therefore, at the translational level, *Emilin1* deficiency results in increased fibrogenesis accompanied by alterations in immune function and age-associated remodeling, and these alterations occur at the same time as micro level and before macro level biomechanical dysfunction.

***Emilin1* deficiency results in enrichment of unique pathways associated with AV disease**

Pathway enrichment was utilized to earmark pathways influenced by *Emilin1* deficiency (Figure 3B, gene annotation and statistics in Supplementary Table 1B). Multiple changes in signaling pathways occurred coincident with the progressive stiffening observed by

biomechanical testing. The EGFR1 signaling pathway, associated with endothelial dysfunction and cardiac remodeling,^{28,29} showed increased pathway enrichment in *Emilin1*^{-/-} mice versus WT (Supplemental Table 1B). The PPAR signaling pathway, known to protect against cardiovascular calcification,³⁰ showed an increase in enrichment in the aged *Emilin1*^{-/-} AV relative to other valve proteomes. “Apoptosis” was not significantly enriched in the adult WT mice but appeared enriched in all other groups, suggesting that apoptosis is a process of normal aging that is accelerated by *Emilin1* deficiency. While AV tissue in adult WT showed a low level of enrichment for VEGF and adult *Emilin1*^{-/-} showed no significant enrichment for VEGF pathways, AV tissue in the aged WT and aged *Emilin1*^{-/-} showed significant enrichment of VEGF signaling, which is consistent with previous observations.¹² The mTOR pathway, critical to the regulation of inflammation and complex immune responses during hemodynamic stress^{31,32}, was significantly enriched in the aged *Emilin1*^{-/-} AV only. Overall, these findings report that *Emilin1* deficiency influences changes in multiple signaling pathways simultaneous with microscale AV stiffening that precedes macroscale biomechanical alterations.

Altered protein networks in *Emilin1*^{-/-} mice indicate an early AV disease process and demonstrate increased aberrancy over time coincident with disease progression

Significantly altered protein expression was further analyzed for primary biological functions, comparing WT and *Emilin1*^{-/-} during aging. Bioinformatics analysis showed that altered proteins affected filament and myofibril formations, morphology of cells, and apoptosis (Figure 4A, Supplemental Table 3). Proteins involved in both the formation of myofibrils (MYH6, MYL2, PKP2, TTN) and filaments (MYOMI, PKP2, TTN) decreased with the exception of STAT3, which increased. Cell death and apoptosis were increased in adult *Emilin1*^{-/-} mice compared to adult WT. Importantly, EMILIN1 protein was obliterated at both ages, consistent with null expression of the gene. In previous work (Munjal et al, 2014), we showed that several myofibril components are altered in the *Emilin1* deficient aortic valve, including upregulation of the markers SMA, SMemb and SM22. Likewise, we documented increased apoptosis in the *Emilin1*^{-/-} mutant aortic valve using cleaved caspase-3 immunohistochemistry. The current proteomic data reports that multiple proteins are altered by the absence of EMILIN1, proteins that contribute to the formation of myofibrils and filaments, as well as the regulation of programmed cell death (apoptosis). Thus perturbation of myofibril processes and multiple maladaptive compensatory effects are observed at the translational level due to aging in the *Emilin1*^{-/-} AV.

In the aged *Emilin1*^{-/-} valves, protein networks impacting cell proliferation were notably changed compared to the adult *Emilin1*^{-/-} AV (Figure 4B). A majority of the related proteins (22/30, 73%) were increased in aged *Emilin1*^{-/-} AVs. In this subset of altered proteins, there were significant differences showing dysregulated adhesion and immune responses. In addition, there was derangement of proteins and processes involved in cytoskeletal organization, consistent with previous observations describing the role of VIC activation in AV disease pathogenicity.¹² Immune cell adhesion proteins (PECAM1, MYO1G, MRC1) were elevated compared to WT littermates, with decreases in proteins SRC and MYADM. Interestingly, FBLN5, associated with inhibition of angiogenesis³³, was

decreased in the aged *Emilin1*^{-/-} compared to WT, suggesting that EMILIN1-FBLN5 interactions may have a role in the increased angiogenesis detected at the proteomic level, consistent with the increase in aberrant angiogenesis detected in AV disease progression.³⁴ Overall, the adult *Emilin1*^{-/-} AV showed dysregulation related primarily to cellular organization and fibril maintenance, while the aged *Emilin1*^{-/-} AV shows differences in protein expression related to increased proliferation, aberrant angiogenesis and immune dysregulation.

Cell adhesion and fibronectin binding are altered in the context of *Emilin1* deficiency and aging

A small subset of proteins was altered when comparing the adult and aged *Emilin1*^{-/-} mutants (Figure 5A, B). ECM organization was the main process interrupted. Collagens 4a3 and 6a5 were increased in the aged compared to adult *Emilin1*^{-/-} mice, and were linked to the Gene Ontology function of “ECM organization.” The aged *Emilin1*^{-/-} AV was characterized also by abnormal cell adhesion, through increased COL4A3 and COL6A5, and decreased CCDC80 and PPAP2B. FN1 was not significantly altered in any group comparison. These changes likely reflect early primary structural changes to the valve scaffold in response to *Emilin1* deficiency and different secondary changes in the older mouse.

Aged WT AVs (AgWT/AdWT) showed increased cell activation, immune response, and adhesion (Figure 5C), including increases in the proteins vitronectin (VTN, secreted protein associated with maintenance of valve integrity)^{35,36}, VCAM1 (marker of inflammation), and FBLN1 (modulator of OFT endothelial mesenchymal transition)³⁷, identifying multiple processes involved in alteration of AV structure. Overall, these findings are consistent with the observation that age is an independent risk factor for developing AV disease and that normal aging processes contribute to the pathogenesis of AV disease.

***Emilin1* deficiency affects ECM proteins downstream of TGFB1 signaling**

Since previous work demonstrated that non-canonical TGFB1 signaling contributes to AVD pathogenesis¹², we examined proteins interactive with TGFB1 signaling. Calculation of the primary local network surrounding EMILIN1, ELASTIN and TGFB1 showed complex interactions using proteomics (Figure 6A). Proteins within this network contribute to structural integrity of valve tissue and therefore impact organization and durability, ultimately effecting valve function and resulting in disease. Trend analysis showed which proteins paralleled or diverged from EMILIN1 levels (Figure 6B). Proteins that were simultaneously decreased in the *Emilin1* deficient mouse included cartilage intermediate layer protein (CILP1), growth differentiation factor 11 (GDF11, also known as BMP11), and FIBULIN1. Conversely, ECM proteins that increased with *Emilin1* deficiency over time included WNT9B and COL6A5. The latent transforming growth factor beta binding protein 3 (LTBP3) and fibulin-5 (FBLN5) protein were decreased in aged *Emilin1*^{-/-} mice. EMILIN1 protein is primarily localized to the ventricularis layer of the WT valve cusp, and protein expression is obliterated in *Emilin1*^{-/-} mice (Figure 7A). EMILIN1 protein content and localization has not been reported in healthy or diseased human heart valves. Additional experiments confirmed that *Emilin1* deficiency results in decreased LTBP3, FBLN5 and

CILP1 in aged AV tissue (Figure 7). Overall, these findings identify new downstream effects of EMILIN1 signaling that link TGFB1 signaling and aberrant ECM expression, further showing that EMILIN1 has a broad and diverse role in maintaining the structural integrity of AVs.

Discussion

In the current study, proteomic composition was examined in relationship to biomechanical properties in the context of *Emilin1* deficiency and aging. The *Emilin1* deficient mouse has been characterized as a model of latent AV disease with pathogenesis primarily related to ECM defects and altered non-canonical TGFB1 signaling.¹² We report that biomechanical measurements are associated with translational level changes, and patterns of misexpression of specific biologic processes and signaling pathways are associated with early AV disease processes, prior to the manifestation of overt disease. Strengths of this study are the analyses of aggregate protein profile in a model of aortic valve disease before and after disease onset, and the correlation of this comprehensive description to measures of valve function. These findings provide important information about pathologic changes that occur in early stages of disease, and provide patterns of disease progression that may provide insight into human AV disease and mechanisms of aging.

To our knowledge this is the first time that biomechanical functional studies have been performed with proteomic expression analysis during AV disease progression. Biomechanical measurements by two modalities indicate that EMILIN1 deficiency is associated with significant changes in tissue stiffness at both the macro and micro scales in the aged mouse, correlating with the manifestation of hemodynamically significant disease.¹² Aging in the context of *Emilin1* deficiency resulted in macro level stiffening of both cusp and annulus regions, as well as proteomic processes, including inflammation, immune infiltration and fibrosis. Interestingly, testing at the micro level also shows biomechanical perturbations due to *Emilin1* deficiency in the adult cusp before pathological signs of AV disease. In the adult AV cusp, proteomic changes in pathway signaling and biological function were concomitant with altered biomechanical properties. We suggest that EMILIN1 is necessary for biomechanical stability of the healthy AV cusp and that loss of EMILIN1 accelerates the maladaptive biomechanical effects of the aging process primarily through premature ECM abnormalities. Importantly, this study shows that two modalities of measuring tissue stiffness are in agreement, but that AFM has increased sensitivity to identify more subtle changes. This study identifies that altered protein expression is associated with significant biomechanical changes that worsen at the microscale level and contribute to progressive degeneration of valve tissue.

Previous work demonstrated that *Emilin1*^{-/-} AV structure deteriorates prior to dysfunction, and advanced AV disease processes, including inflammation and fibrosis, occur later in the context of hemodynamic disease.¹² In our current work, we focused on proteomic analyses of the AV cusp as there is no reliable way to dissect the amount of annulus material needed for proteomic studies. Here, proteomic analysis showed similar enrichment of inflammatory response among all four proteomes, but with differentiating immune processes (Figure 3A). This suggests that at the global protein level, normal aging of the valvular structure involves

similar inflammatory regulation that is not affected by *Emilin1* deficiency. We suggest that proteins clustered to “inflammatory response” may collectively participate in fundamental AV homeostasis, including proteins that contribute to normal AV development but also intersect with injury-induced inflammatory processes, and may or may not be sufficient to cause pathological changes. Instead, pathological AV structural changes at the global proteomic level appear to involve increased immune processes in combination with specific inflammatory processes that are present in the aged *Emilin1* deficient mouse. This is further supported by the new pathway information involved in EMILIN1 expression (Figure 3B), namely the mTOR, EGFR1 and the PPAR γ pathways, suggesting complex regulation of homeostasis and pathogenesis.

The mTOR pathway has multiple roles in cardiac adaptability by controlling protein turnover through targets of rapamycin^{38,39}, and modifies inflammatory response through regulation of immunoproteasomal degradation under hemodynamic stress.³¹ We hypothesize that the proteomic enrichment of the mTOR pathway in the aged *Emilin1*^{-/-} AV suggests that mTOR signaling may regulate an immune mechanism that modifies inflammatory processes and ultimately contributes to the progression of AV disease. The role of mTOR in resident immune cells is complex and activation of this pathway may have variable inflammatory responses.⁴⁰ The EGFR1 and PPAR pathways showed increased enrichment in both adult and aged *Emilin1*^{-/-} AVs compared to WT, suggesting these molecular changes occurred before biomechanical dysfunction or the effects of aging. Both pathways are known to have a fundamental role in the structural integrity of valve tissue. The EGFR tyrosine kinase receptor is required for appropriate AV development, and regulates proliferation of mesenchymal cells during cushion remodeling.²⁹ EGFR works to suppress BMP signaling, and primary osteoblasts from *Egfr*^{-/-} mice show increased formation of calcific bone nodules relative to controls, showing a role for EGFR in limiting processes of calcification⁴¹. In valve tissue, loss of EGFR causes strain specific AV hyperplasia and AV structure thickening leading to stenosis and calcification.⁴² *Emilin1*^{-/-} mice do not show development of calcific nodules, therefore, the *Emilin1*^{-/-} proteomic increases in enrichment of EGFR signaling may reflect activation of mechanisms surrounding the lack of calcification in this model. This is a novel insight provided by the proteomic data and further work is needed to completely delineate these mechanisms. PPAR γ has protective anti-calcific effects in valve tissue through upstream regulation of osteopontin.^{43,44} Increases in EGFR1 and PPAR γ pathways may contribute to disease progression but paradoxically prevent calcification in *Emilin1*^{-/-} valves. The results from the current study suggest multiple inflammatory pathways may contribute to disease and these pathways could provide new therapeutic targets by blocking maladaptive inflammation prior to advance disease states.

Emilin1 deficiency has been linked to both canonical and non-canonical TGFB1 signaling in aged AV tissue.¹² We have expanded these observations by demonstrating that *Emilin1* inactivation reduces expression of multiple ECM proteins in the EMILIN1-TGFB1 network, better defining the downstream structural and functional effects of *Emilin1* deficiency (Figure 6). All direct methods for protein-to-protein interaction annotation use the common principle that proteins that interact with each other are more likely to show similar expression patterns upon phenotypic modulation.⁴⁵ This is referred to as the modularity of

disease.⁴⁶ Here, the data from the ECM proteins LTBP3, FBLN5, CILP1, established factors in AVD progression, suggests that these proteins have functional protein-to-protein interactions with EMILIN1 as defined by similarities in expression patterns at all time points (CILP1) or in aged *Emilin1*^{-/-} AV (LTBP3 and FBLN5). *Emilin1* deficiency in the aged AV resulted in marked decreases of LTBP3, FBLN5, and CILP1. LTBP3 is capable of binding all three TGF β isoforms, but its relationship to TGF β 1 is less well known.⁴⁷ LTBP3 deficiency in mice is associated with decreased TGF β 1 signaling,⁴⁸ but the valves of these mice have not been studied. LTBP3 increased in the adult *Emilin1*^{-/-} AV but decreased in the aged *Emilin1*^{-/-} AV, suggesting that LTBP3-TGF β 1 interactions are dynamically modulated. This is supported by reports that LTBP3 is capable of differentially regulating TGF β 1 signaling.^{49,50} FBLN5 is essential for elastic fiber development through sequestration of TGF β 1, and patients homozygous for a missense mutation in *FBLN5* have cutis laxa, a skin disease, and show thickened aortic valves with supravalvular aortic stenosis.⁵¹ The current data suggest that EMILIN1 interactions may play a significant role in FBLN5 modulation of TGF β 1. Finally, CILP1 was effectively eliminated in both adult and aged *Emilin1*^{-/-} AVs. CILP1 acts to suppress IGF1-induced proliferation⁵² and inhibits transcriptional activation of cartilage genes through TGF β 1.⁵³ *Emilin1* deficiency has been shown to have increased proliferative effects.¹² The combination of proteomic and biomechanical data suggests that excessive proliferation may be the result of loss of CILP1. Taken together, the data suggest that the EMILIN1-TGF β 1 interactions influence a variety of proteins and protein networks that regulate valve structure and function and contribute to disease progression.

This study has notable limitations. *Emilin1* deficiency results in systemic hypertension, which may result in cardiac remodeling over time. The *Emilin1*^{-/-} mouse has been carefully characterized with highly penetrant (100% of mice in the seminal study) systemic hypertension as measured both invasively and non-invasively.¹⁴ We have confirmed the same penetrance and severity of hypertension in our colony of mice, but did not measure blood pressure in the mice used in this study. While AV dysfunction also results in cardiac remodeling, it is unknown if mechanisms of cardiac dysfunction could cause or exacerbate valve dysfunction. It is possible that proteomic effects in *Emilin1*^{-/-} AV could involve some compensation for global loss of EMILIN1. Proteomics was performed on the cusp and hinge and did not include a large amount of annulus. Annulus tissue alone is difficult to isolate by the microdissection methods needed for proteomic studies and may be associated with large amounts of aortic wall tissue, which would contaminate the valvular proteome. Some limitations in the proteomic work are due to processes inherent with shotgun proteomic sampling. Proteomic studies capture only the top ~35% of the entire proteomes due to dynamic sampling by mass spectrometry.⁵⁴ Increasing the number of technical replicates per biological sample increases the detection of low count proteins⁵⁴, but performing extensive replicates is limited by sample availability and cost. Scaffold ECM proteins may be missing from the analysis, including various predictable elastic fiber proteins and proteoglycans. This is because the discussed proteomes were obtained by decellularization processes,²¹ which leaves behind bound scaffold proteins. However, these studies provide information that will direct future studies to target specific scaffold proteins to further elucidate ECM modifications occurring during AV disease progression.

EMILIN1 is necessary for maintenance of normal AV structure and function. *Emilin1* deficiency results in early ECM structural disorganization and disruption of ECM cell signaling, which can be detected functionally at the micro level before hemodynamic disease. Late activation of protein networks results in increased proliferation, inflammation and fibrosis, as well as a complex immune response, which collectively results in both micro and macro biomechanical dysfunction at the time of overt hemodynamic AV disease (Figure 8). This is shown in established histopathological changes characterizing this model.^{12,27} Multiple signaling pathways are altered before overt disease manifestation, including mTOR, EGFR1 and PPAR γ pathways, suggesting a complex role for inflammatory and immune mediated responses. EMILIN1 interacts with TGFB1, a primary controller of AV disease progression, and the protein network associated with this interaction has identified new protein relationships that may inform AV structure and function. EMILIN1 interaction networks have a significant impact on ECM composition and intrinsic biomechanical properties that influence valve function over time. This study increases our understanding of markers of aging in the context of early AV disease processes, a necessary step to elucidating the contribution of aging to AV disease pathogenesis. EMILIN1 is an important modifier of AV disease progression. Taken together, EMILIN1 impacts proteins involved in disease initiation and progression, as well as processes involved in advanced disease. Defining early patterns of protein changes during early stages of disease may provide new predictive biomarkers to monitor disease progression or therapeutic targets.

Supplementary Material

Refer to Web version on PubMed Central for supplementary material.

Acknowledgments

We thank Aaron Reed for help in microscopy work and Susana Comte-Walters for help in proteomics data analysis. This study was supported by the National Center for Advancing Translational Sciences of the NIH (P.M.A., UL1 TR000445), National Institute of General Medical Sciences (P.M.A., P20 GM103542-06) the National Heart Lung and Blood Institute of the NIH (R.B.H., HL117851) an Institutional Clinical and Translational Science Award (R.B.H., NIH/NCRR 8UL1TR000077), and the Cincinnati Children's Research Foundation (R.B.H.).

Abbreviations

AFM	atomic force microscopy
AV	aortic valve
ECM	extracellular matrix
TGFB1	transforming growth factor beta 1
VIC	valve interstitial cell
WT	wild type

References

1. Nkomo VT, et al. Burden of valvular heart diseases: A population-based study. *The Lancet*. 2006; 368(9540):1005–1011.

2. Aronow WS. Valvular aortic stenosis in the elderly. *Cardiology in Review*. 2007; 15(5):217–225. [PubMed: 17700380]
3. Moremen KW, Tiemeyer M, Nairn AV. Vertebrate protein glycosylation: Diversity, synthesis and function. *Nature Reviews Molecular Cell Biology*. 2012; 13(7):448–462. [PubMed: 22722607]
4. Merryman WD, Schoen FJ. Mechanisms of calcification in aortic valve disease: Role of mechanokinetics and mechanodynamics. *Current Cardiology Reports*. 2013; 15(5):1–7.
5. Aikawa E, et al. Human semilunar cardiac valve remodeling by activated cells from fetus to adult: Implications for postnatal adaptation, pathology, and tissue engineering. *Circulation*. 2006; 113(10):1344–1352. [PubMed: 16534030]
6. Hinton RB Jr, et al. Extracellular matrix remodeling and organization in developing and diseased aortic valves. *Circulation Research*. 2006; 98(11):1431–1438. [PubMed: 16645142]
7. Wirrig EE, Hinton RB, Yutzey KE. Differential expression of cartilage and bone-related proteins in pediatric and adult diseased aortic valves. *Journal of Molecular and Cellular Cardiology*. 2011; 50(3):561–569. [PubMed: 21163264]
8. Krishnamurthy VK, et al. Maladaptive matrix remodeling and regional biomechanical dysfunction in a mouse model of aortic valve disease. *Matrix Biology*. 2012; 31(3):197–205. [PubMed: 22265892]
9. Alvarez-Llamas G, et al. Modification of the secretion pattern of proteases, inflammatory mediators, and extracellular matrix proteins by human aortic valve is key in severe aortic stenosis. *Molecular & Cellular Proteomics*. 2013; 12(9):2426–2439. [PubMed: 23704777]
10. Martín-Rojas T, et al. Proteomic profile of human aortic stenosis: Insights into the degenerative process. *Journal of Proteome Research*. 2012; 11(3):1537–1550. [PubMed: 22276806]
11. Miller JD, Weiss RM, Heistad DD. Calcific aortic valve stenosis: Methods, models, and mechanisms. *Circulation Research*. 2011; 108(11):1392–1412. [PubMed: 21617136]
12. Munjal C, et al. Tgf- β mediates early angiogenesis and latent fibrosis in an emilin1-deficient mouse model of aortic valve disease. *Disease Models & Mechanisms*. 2014; 7(8):987–996. [PubMed: 25056700]
13. Zanetti M, et al. Emilin-1 deficiency induces elastogenesis and vascular cell defects. *Molecular and Cellular Biology*. 2004; 24(2):638–650. [PubMed: 14701737]
14. Zacchigna L, et al. Emilin1 links tgfbeta maturation to blood pressure homeostasis. *Cell*. 2006; 124(5):929–942. [PubMed: 16530041]
15. Rajamannan NM, et al. Calcific aortic valve disease: Not simply a degenerative process a review and agenda for research from the national heart and lung and blood institute aortic stenosis working group executive summary: Calcific aortic valve disease: 2011 update. *Circulation*. 2011; 124(16):1783–1791. [PubMed: 22007101]
16. Krishnamurthy VK, Guilak F, Narmoneva DA, Hinton RB. Regional structure-function relationships in mouse aortic valve tissue. *J Biomech*. 2011; 44(1):77–83. [PubMed: 20863504]
17. Jones WR, et al. Alterations in the young's modulus and volumetric properties of chondrocytes isolated from normal and osteoarthritic human cartilage. *J Biomech*. 1999; 32(2):119–27. [PubMed: 10052916]
18. Theret DP, Levesque MJ, Sato M, Nerem RM, Wheeler LT. The application of a homogeneous half-space model in the analysis of endothelial cell micropipette measurements. *J Biomech Eng*. 1988; 110(3):190–9. [PubMed: 3172738]
19. Guilak F, Alexopoulos LG, Haider MA, Ting-Beall HP, Setton LA. Zonal uniformity in mechanical properties of the chondrocyte pericellular matrix: Micropipette aspiration of canine chondrons isolated by cartilage homogenization. *Ann Biomed Eng*. 2005; 33(10):1312–8. [PubMed: 16240080]
20. Sewell-Loftin MK, Brown CB, Baldwin HS, Merryman WD. A novel technique for quantifying mouse heart valve leaflet stiffness with atomic force microscopy. *J Heart Valve Dis*. 2012; 21:513–520. [PubMed: 22953681]
21. Angel PM, et al. Networked-based characterization of extracellular matrix proteins from adult mouse pulmonary and aortic valves. *Journal of Proteome Research*. 2011; 10(2):812–823. [PubMed: 21133377]

22. Zhang B, Kirov S, Snoddy J. Webgestalt: An integrated system for exploring gene sets in various biological contexts. *Nucleic acids research*. 2005; 33(Web Server Issue):W741. [PubMed: 15980575]
23. Duncan D, Prodduturi N, Zhang B. Webgestalt2: An updated and expanded version of the web-based gene set analysis toolkit. *BMC Bioinformatics*. 2010; 11(Suppl 4):P10.
24. Benjamini Y, Hochberg Y. Controlling the false discovery rate: A practical and powerful approach to multiple testing. *Journal of the Royal Statistical Society. Series B (Methodological)*. 1995; 57(1):289–300.
25. Saeed AI, et al. Tm4 microarray software suite. *Methods in Enzymology*. 2006; 411:134–193. [PubMed: 16939790]
26. Pezet M, et al. Elastin haploinsufficiency induces alternative aging processes in the aorta. *Rejuvenation Research*. 2008; 11(1):97–112. [PubMed: 18173368]
27. Munjal C, et al. Inhibition of mapk-erk pathway in vivo attenuates aortic valve disease processes in emilin1-deficient mouse model. *Physiological Reports*. 2017; 5(5):e13152. [PubMed: 28270590]
28. Makki N, Thiel KW, Miller FJ. The epidermal growth factor receptor and its ligands in cardiovascular disease. *International Journal of Molecular Sciences*. 2013; 14(10):20597–20613. [PubMed: 24132149]
29. Iwamoto R, Mekada E. Erbb and hb-egf signaling in heart development and function. *Cell Structure and Function*. 2006; 31(1):1–14. [PubMed: 16508205]
30. Chu Y, et al. Pioglitazone attenuates valvular calcification induced by hypercholesterolemia. *Arteriosclerosis, Thrombosis, and Vascular Biology*. 2013; 33(3):523–532.
31. Xu L, Brink M. Mtor, cardiomyocytes and inflammation in cardiac hypertrophy. *Biochimica et Biophysica Acta (BBA)-Molecular Cell Research*. 2016 pii: S0167-4889(16)00006-9.
32. Weichhart T, Hengstschläger M, Linke M. Regulation of innate immune cell function by mtor. *Nature Reviews Immunology*. 2015; 15(10):599–614.
33. Sullivan KM, Bissonnette R, Yanagisawa H, Hussain SN, Davis EC. Fibulin-5 functions as an endogenous angiogenesis inhibitor. *Laboratory investigation*. 2007; 87(8):818–827. [PubMed: 17607303]
34. Yoshioka M, et al. Chondromodulin-i maintains cardiac valvular function by preventing angiogenesis. *Nature Medicine*. 2006; 12(10):1151–1159.
35. Akhtar S, Meek KM, James V. Immunolocalization of elastin, collagen type i and type iii, fibronectin, and vitronectin in extracellular matrix components of normal and myxomatous mitral heart valve chordae tendineae. *Cardiovascular Pathology*. 1999; 8(4):203–211. [PubMed: 10724524]
36. Wiltz, D., et al. Extracellular matrix organization, structure, and function. In: Aikawa, E., editor. *Calcific aortic valve disease*. 2013. InTech
37. Harikrishnan K, et al. Fibulin-1 suppresses endothelial to mesenchymal transition in the proximal outflow tract. *Mechanisms of Development*. 2015; 136:123–132. [PubMed: 25575930]
38. Balasubramanian S, et al. Mtor in growth and protection of hypertrophying myocardium. *Cardiovascular & Hematological Agents in Medicinal Chemistry (Formerly Current Medicinal Chemistry-Cardiovascular & Hematological Agents)*. 2009; 7(1):52–63.
39. Hwang S-K, Kim H-H. The functions of mtor in ischemic diseases. *BMB reports*. 2011; 44(8): 506–511. [PubMed: 21871173]
40. Varki A. Biological roles of glycans. *Glycobiology*. 2017; 27(1):3–49. [PubMed: 27558841]
41. Sabilia M, et al. Mice humanised for the egf receptor display hypomorphic phenotypes in skin, bone and heart. *Development*. 2003; 130(19):4515–4525. [PubMed: 12925580]
42. Barrick CJ, et al. Reduced egfr causes abnormal valvular differentiation leading to calcific aortic stenosis and left ventricular hypertrophy in c57bl/6j but not 129s1/svimj mice. *American Journal of Physiology-Heart and Circulatory Physiology*. 2009; 297(1):H65–H75. [PubMed: 19448146]
43. Steitz SA, et al. Osteopontin inhibits mineral deposition and promotes regression of ectopic calcification. *The American Journal of Pathology*. 2002; 161(6):2035–2046. [PubMed: 12466120]
44. Li F, et al. Pioglitazone attenuates progression of aortic valve calcification via down-regulating receptor for advanced glycation end products. *Basic Research in Cardiology*. 2012; 107(6):1–14.

45. Sharan R, Ulitsky I, Shamir R. Network-based prediction of protein function. *Molecular Systems Biology*. 2007; 3(1)
46. Jiang X, et al. Modularity in the genetic disease-phenotype network. *FEBS Letters*. 2008; 582(17): 2549–2554. [PubMed: 18582463]
47. Robertson IB, et al. Latent $\text{tgf-}\beta$ -binding proteins. *Matrix Biology*. 2015; 47:44–53. [PubMed: 25960419]
48. Dabovic B, et al. Bone abnormalities in latent $\text{tgf-}\beta$ binding protein (Itbp)-3-null mice indicate a role for Itbp-3 in modulating $\text{tgf-}\beta$ bioavailability. *The Journal of Cell Biology*. 2002; 156(2):227–232. [PubMed: 11790802]
49. Vehviläinen P, et al. Latent $\text{tgf-}\beta$ binding proteins (Itbps) 1 and 3 differentially regulate transforming growth factor- β activity in malignant mesothelioma. *Human Pathology*. 2011; 42(2): 269–278. [PubMed: 21106222]
50. Koli K, Ryynänen MJ, Keski-Oja J. Latent $\text{tgf-}\beta$ binding proteins (Itbps)-1 and-3 coordinate proliferation and osteogenic differentiation of human mesenchymal stem cells. *Bone*. 2008; 43(4): 679–688. [PubMed: 18672106]
51. Loeys B, et al. Homozygosity for a missense mutation in fibulin-5 (fbln5) results in a severe form of cutis laxa. *Human Molecular Genetics*. 2002; 11(18):2113–2118. [PubMed: 12189163]
52. Johnson K, Farley D, Hu SI, Terkeltaub R. One of two chondrocyte-expressed isoforms of cartilage intermediate-layer protein functions as an insulin-like growth factor 1 antagonist. *Arthritis & Rheumatism*. 2003; 48(5):1302–1314. [PubMed: 12746903]
53. Seki S, et al. Cartilage intermediate layer protein promotes lumbar disc degeneration. *Biochemical and Biophysical Research Communications*. 2014; 446(4):876–881. [PubMed: 24631904]
54. Liu H, Sadygov RG, Yates JR. A model for random sampling and estimation of relative protein abundance in shotgun proteomics. *Analytical Chemistry*. 2004; 76(14):4193–4201. [PubMed: 15253663]

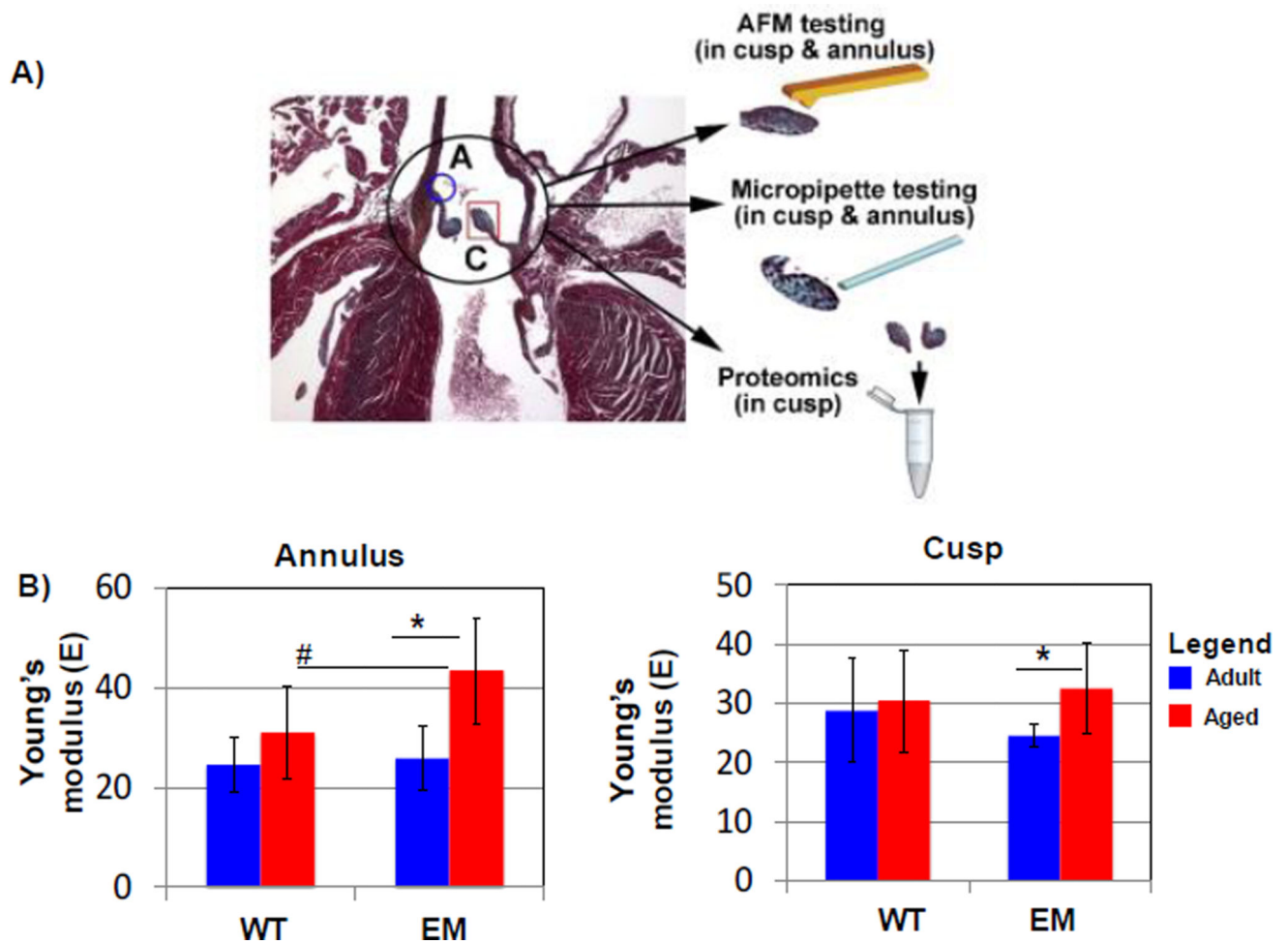


Figure 1. Determination of mechanical stiffness by genotype and age using micropipette biomechanical testing

Micropipette biomechanical characterization (MBC) of the *Emilin1*^{-/-} (EM) on whole mount AVs compared to WT litter mates. A) Valve tissue regions studied by different modalities. B) *Emilin1* deficiency significantly increased AV stiffness in the annulus compared to aged WT littermates and during aging of the *Emilin1*^{-/-} mouse; B) *Emilin1* deficiency increased stiffness in the cusp during aging, with no significant change in WT due to aging. Significant differences were determined using one-way ANOVA *p*-value 0.03. Asterisks denote significant differences when comparing ages; Hashtags denote significant differences when comparing genotypes. AdWT- adult wild type; AgWT- aged wild type; AdEM, adult *Emilin1*^{-/-}, AgEM, aged *Emilin1*^{-/-}.

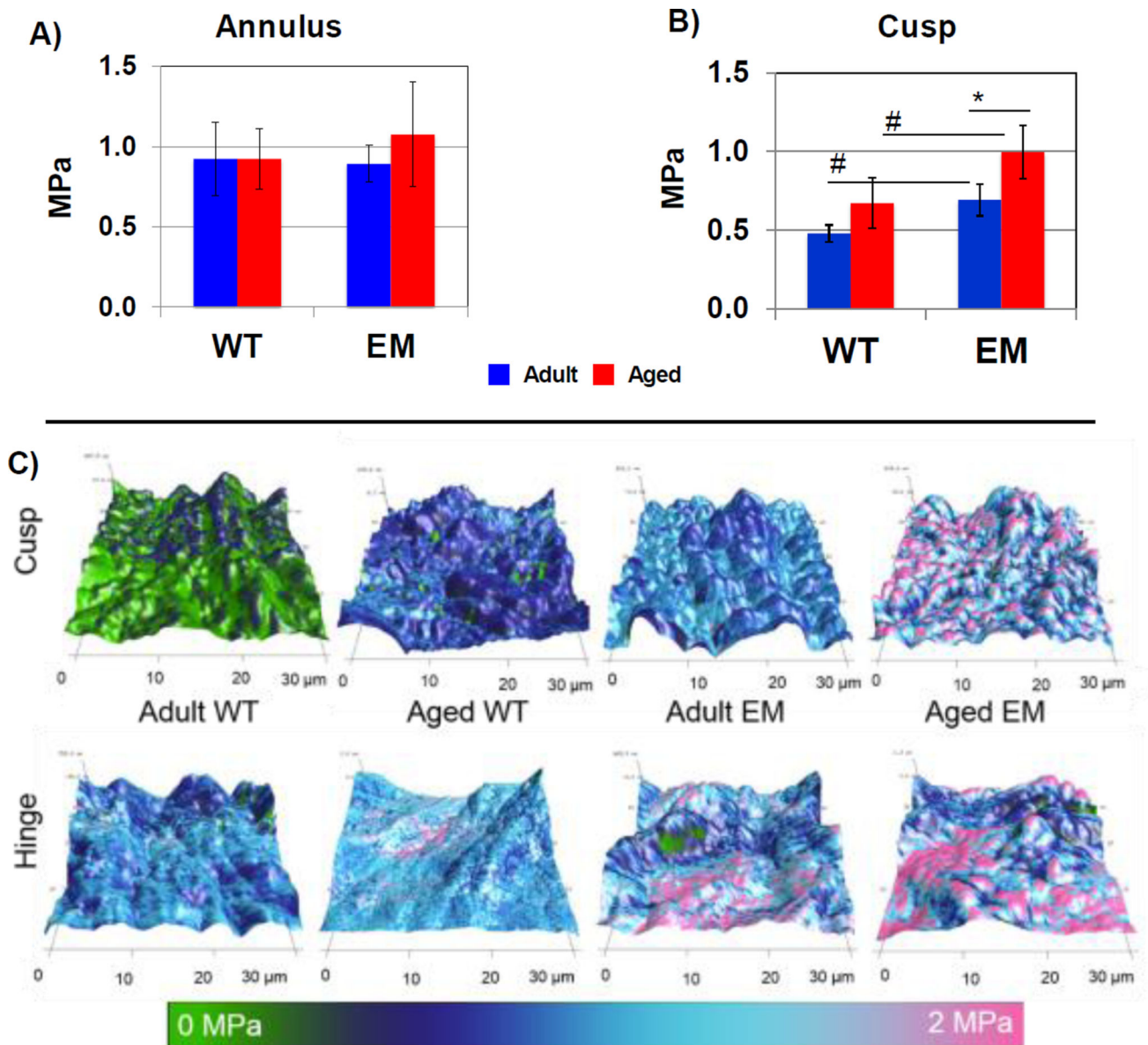


Figure 2. Determination of mechanical stiffness by genotype and age using atomic force microscopy

AFM of AV cusp cross sections ($30 \times 30 \mu\text{m}^2$ measurement areas). A) Annulus region did not show a significant difference in microscale cross sectional measurements. B) AFM showed a significant increase in microenvironmental cusp stiffness between WT and *Emilin1*^{-/-} at 4 months and 12 months, and when comparing *Emilin1*^{-/-} mice at 4 months and 12-months. C) AFM topography of $30 \times 30 \mu\text{m}$ cross sections, where z-axis shows thickness distribution, and color represents stiffness distribution used to calculate the average values presented in (B). Significant differences were determined using one-way ANOVA p -value < 0.01 . Asterisks denote significant differences when comparing ages; Hashtags denote significant differences when comparing genotypes.

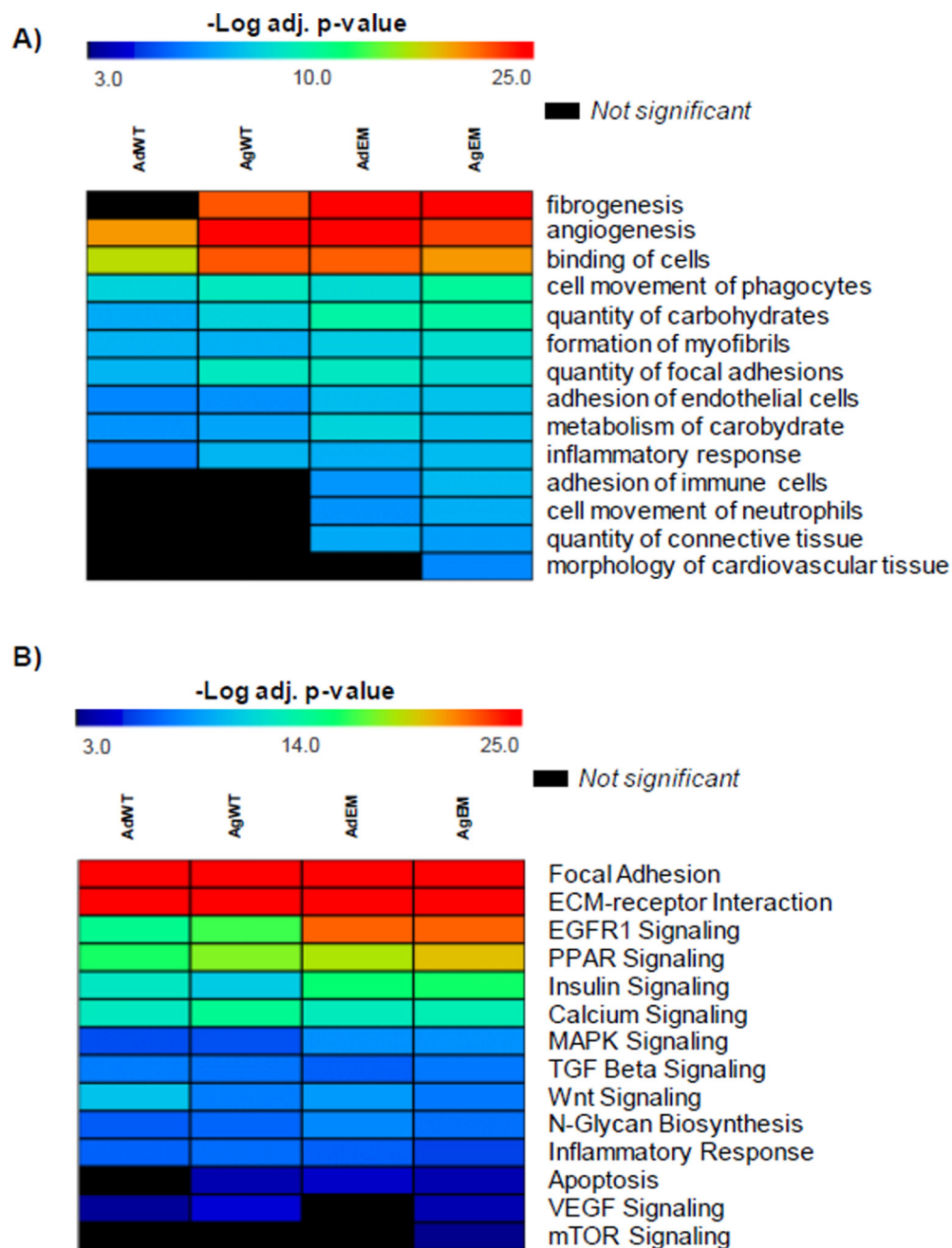


Figure 3. Heat maps for overall proteomic comparison of *Emilin1*^{-/-} and WT aortic valves before and after disease manifestation
 Heat maps of functions and pathways from overall proteomic comparison of adult and aged *Emilin1*^{-/-} and wild type AVs. A) Differential biological functions and processes across each of the 4 proteomes; B) Pathway enrichment from each proteome. All functions and pathways utilize negative log Fisher’s Exact $p\text{-value} = 1.0\text{E-}3$ for statistical significance as shown on the heat map. Red is highest enrichment, blue indicates lower but significant enrichment. Black colored functions are not significant. AdWT - adult wild type; AgWT - aged wild type; AdEM - adult *Emilin1*^{-/-}; AgEM - aged *Emilin1*^{-/-}.

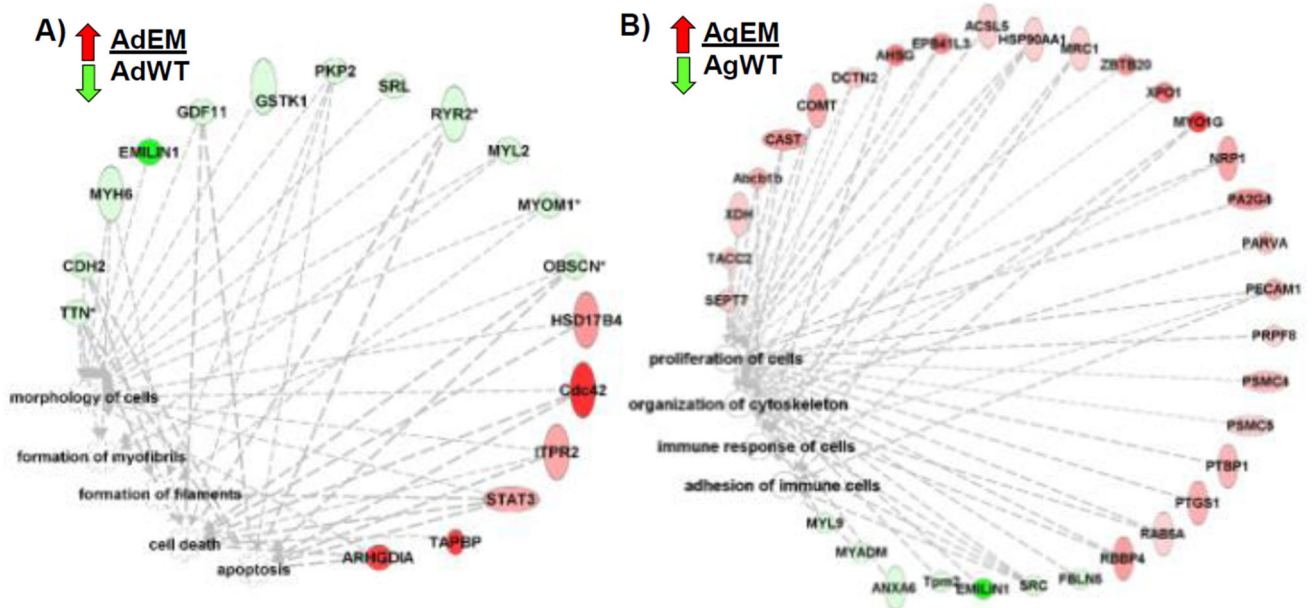


Figure 4. Protein network of significant functions regulated due to *Emilin1* deficiency
 A) Ratio of adult *Emilin1*^{-/-} (AdEM) to adult wild type (AdWT). B) Ratio of aged *Emilin1*^{-/-} (AgEM) to aged WT (AgWT). EMLIN1 was not detected in the *Emilin1*^{-/-} AV. Protein alterations were detected as greater than 2-fold change, *p*-value ≤ 0.05 . IPA analysis log threshold of *p*-value ≤ 3.0 .

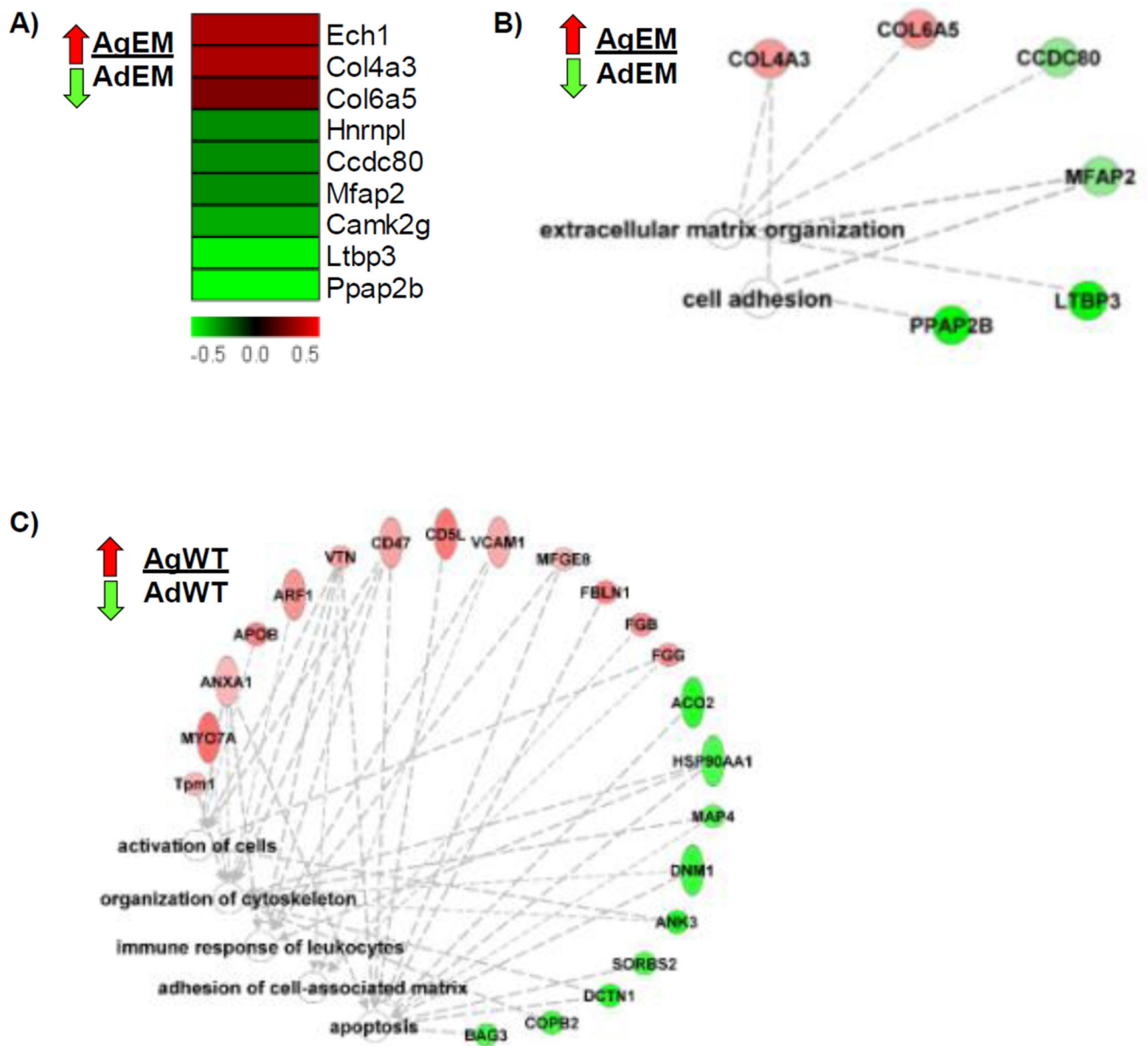


Figure 5. Comparison of aging processes in *Emilin1* deficient or wild type AV tissue
 A) Protein changes in the aging *Emilin1*^{-/-} represented as a ratio aged *Emilin1*^{-/-} (AgEM) to adult *Emilin1*^{-/-} (AdEM). B) Functional processes of altered proteins for ratio AgEM/AdEM C) Function analysis of ratio aged WT (AgWT) to adult WT (AdWT). Functions are calculated using toppcluster.org and reported as $-\log$ bonferroni adjusted p -values ≥ 3.0 and drawn in Ingenuity Pathways Analysis.

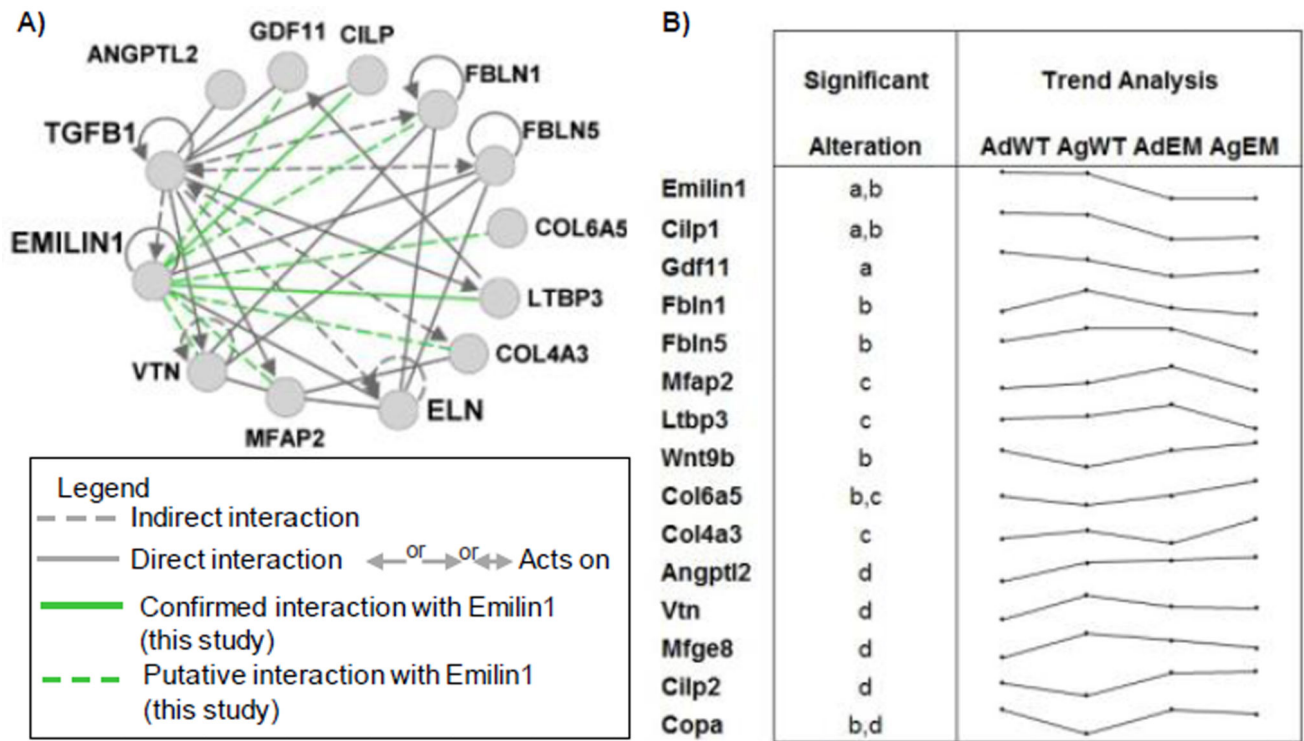


Figure 6. TGFB1-ECM interactive proteins altered by *Emilin1* deficiency or by normal aging
 A) Altered proteins interactive network with TGFB1, ELASTIN and EMILIN1, green lines highlight potential interactions with EMILIN1 as shown by the current study; B) Trend analysis of log transformed spectral counts of ECM proteins showing significant alterations in ratios as tested by p -value < 0.05 : a- *Emilin1*^{-/-} adult/WT adult; b- *Emilin1*^{-/-} aged/WT aged; c- *Emilin1*^{-/-} aged/*Emilin1*^{-/-} adult; d- WT aged/WT adult.

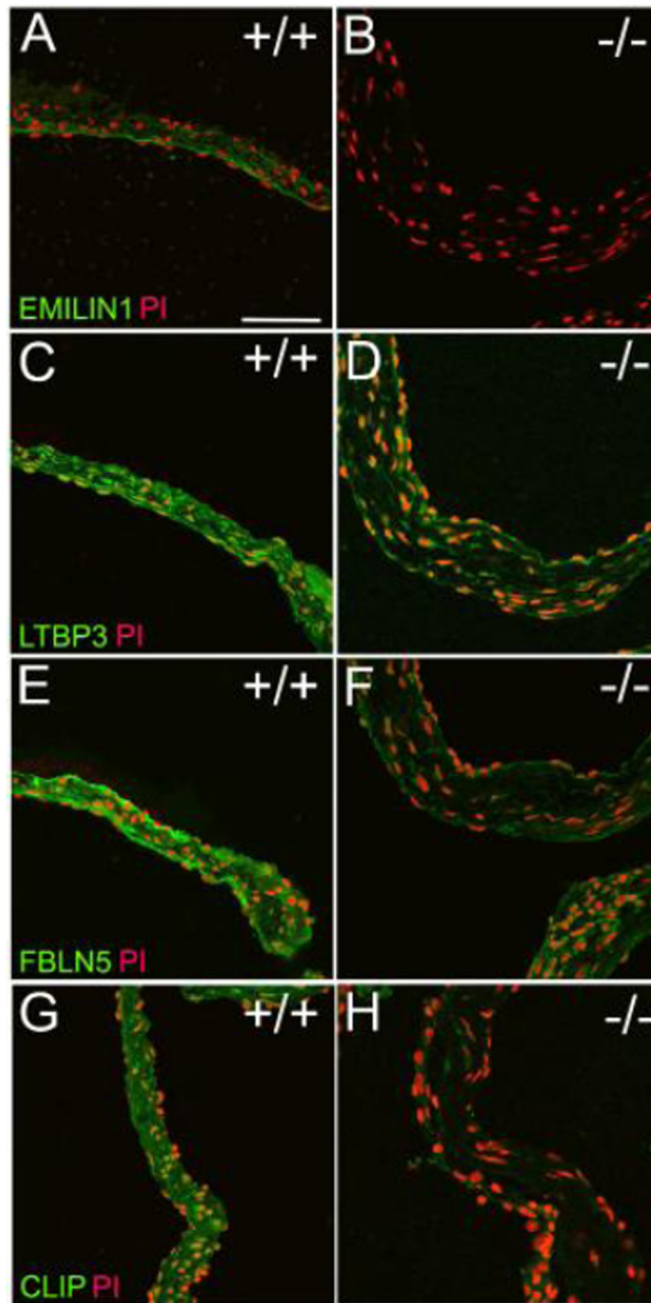


Figure 7. Immunofluorescence confirms that *Emilin1* deficiency reduces expression of multiple ECM proteins in the EMILIN1-TGFB1 interaction network

Comparisons are WT aged AV to *Emilin1*^{-/-} aged AV. A & B) Confirmation of *Emilin1* deficiency in aged AV; LTBP3 (C&D) and FBLN5 (E&F) are significantly decreased in the aged *Emilin1*^{-/-}; CILP1 expression is negligible in aged *Emilin1*^{-/-}.

Emilin1 Deficiency Effects on AV Structure and Function

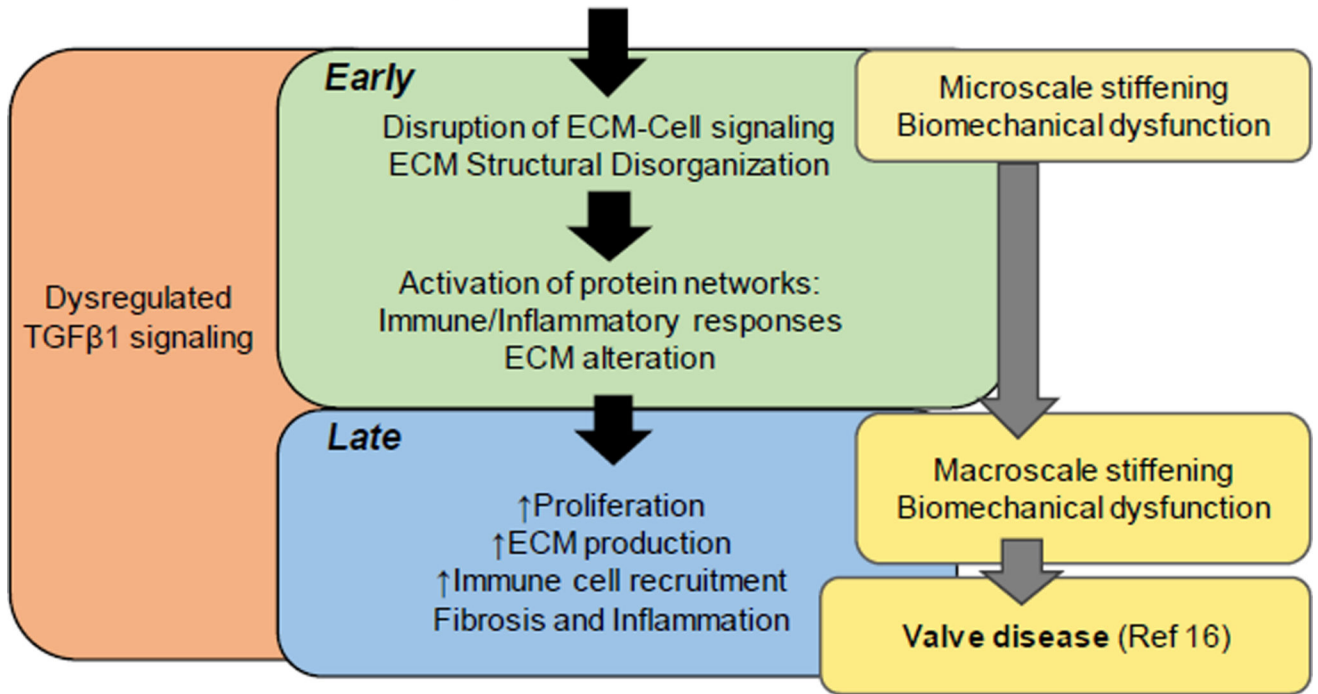


Figure 8. Summary model of the effects of *Emilin1* deficiency in AV disease
 EMILIN1 is an antagonist of TGFβ1.¹⁴ *Emilin1* deficiency results in increased TGFβ1 signaling through canonical pathways involving phosphorylation of Smad2/3 and non-canonical phosphorylation of Erk1/2. This leads to ECM structural disorganization, disruption of ECM-cell networks, and increased protein interactions of inflammation, fibrosis and immune responses in the adult *Emilin1*^{-/-} AV before the manifestation of overt AV disease (Early), which is associated with microscale cusp stiffening. In the aged *Emilin1*^{-/-} AV (Late), ongoing activation of protein networks results in increased proliferation, ECM production and immune recruitment. Increased ECM production leads to overall macroscale tissue-level valve stiffening at the same time that valve dysfunction develops. Observations of early processes improve our understanding of AV disease progression, a necessary step to improve diagnostic and therapeutic tools.